J. Membrane Biol. 134, 169–179 (1993)

The Journal of
Membrane
Biology

Interaction between Red Cell Membrane Band 3 and Cytosolic Carbonic Anhydrase

Gabriela Kifor, Michael R. Toon, Agnes Janoshazi, A.K. Solomon
Biophysical Laboratory, Harvard Medical School, Boston, Massachusetts 02115

Received: 17 July 1992/Revised: 25 January 1993

Abstract. We have previously proposed that a membrane transport complex, centered on the human red cell anion transport protein, band 3, links the transport of anions, cations and glucose. Since band 3 is specialized for HCO_3^-/Cl^- exchange, we thought there might also be a linkage with carbonic anhydrase (CA) which hydrates CO_2 to HCO_3^-. CA is a cytosolic enzyme which is not present in the red cell membrane. The rate of reaction of CA with the fluorescent inhibitor, dansylsulfonamide (DNSA) can be measured by stopped-flow spectrofluorimetry and used to characterize the normal CA configuration. If a perturbation applied to a membrane protein alters DNSA/CA binding kinetics, we conclude that the perturbation has changed the CA configuration by either direct or allosteric means. Our experiments show that covalent reaction of the specific stilbene anion exchange inhibitor, DIDS, with the red cell membrane, significantly alters DNSA/CA binding kinetics. Another specific anion exchange inhibitor, benzene sulfonate (BSate), which has been shown to bind to the DIDS site causes a larger change in DNSA/CA binding kinetics; DIDS reverses the BSate effect. These experiments show that there is a linkage between band 3 and CA, consistent with CA interaction with the cytosolic pole of band 3.

Key words: Red cell — Carbonic anhydrase — Band 3 — Anion exchange protein — Dansylsulfonamide — Anion transport inhibitors

Introduction

Evidence that a membrane transport protein complex is present in the human red cell membrane, where it links the transport of cations to that of anions as well as to glucose uptake, has previously been presented (Janoshazi & Solomon, 1989; Janoshazi, Kifor & Solomon, 1991). The most abundant transmembrane protein, band 3, is the centerpiece of the complex with links both to the membrane-bound Na^+,K^+-ATPase and to the glucose transport protein (GLUT1). Since the primary function of band 3 is the transport of HCO_3^- out of the cell and its exchange for Cl^-, and since the primary role of intracellular carbonic anhydrase (CA) is the hydration of CO_2 to HCO_3^-, we thought that a case could be made for a band 3/CA linkage which would increase efficiency by delivering the processed HCO_3^- directly to band 3 for outward transport. This is particularly important in the human red cell because Randall and Maren (1972) have shown that there is no CA in the membrane. Although there is a very high concentration of CA in the cytoplasm, about 8.6×10^6 cytoplasmic copies of CA/cell (Maren, 1967), there are only about 1.2×10^6 copies of the isozyme, HCA II, which is primarily responsible for the physiological carbonic anhydrase activity (Carter et al., 1984). It is suggestive, and possibly significant, that this number equals the $\approx 1 \times 10^6$ copies of band 3/cell (Jennings, 1989). In the kidney, where CA is essential in maintaining the acid-base balance, Zeidel, Silva and Seifter (1986) have reported that the classical CA inhibitor, acetazolamide (ACTZ), inhibits HCO_3^- efflux in rabbit medullary collecting duct cells which contain a band 3 isoform (Schuster, Bonsib & Jennings, 1986).

The kinetics of CA binding to a specific sulfonamide inhibitor can be measured by stopped-flow spectrofluorimetry, because binding of the fluorescent CA inhibitor, dansylsulfonamide (DNSA), to CA causes both absorption and emission peaks to shift (Chen & Kernohan, 1967). The rationale of our experiments is first to establish the DNSA/CA binding parameters for normal cells and to use these

Correspondence to: A.K. Solomon

parameters to characterize the native CA conformation. When perturbations of band 3 lead to altered DNSA/CA binding kinetics, it follows that the CA binding site conformation has undergone a change, either by direct or allosteric means. We have found that covalent reaction of band 3 with DIDS (4,4'-diisothiocyano-2,2'-stilbene disulfonate), the specific inhibitor of red cell HCO_3^-/Cl^- exchange, modifies DNSA binding kinetics in human red cell pink ghosts. Organic sulfonates, which inhibit red cell anion transport with comparable specificity, though lower affinity (Barzilay, Ship & Cabantchik, 1979), also modify DNSA/CA binding kinetics at concentrations similar to those for anion exchange inhibition; DIDS reverses the organic sulfonate effects. The observation that reaction of band 3 with either of these two specific anion transport inhibitors leads to a modulation of DNSA/CA binding kinetics, indicates that a linkage exists between band 3 and CA, consistent with direct transfer of HCO_3^- between these molecules.

Materials and Methods

Materials

Carbonic anhydrase (BCA II, EC 4.2.1.1.) from bovine red cells (approximate activity 3,000 W-A units/mg protein), *p*-nitrophenyl acetate, dansylsulfonamide (DNSA, 1-dimethylaminonaphthalene-5-sulfonamide), benzene sulfonate, bovine serum albumin and acetazolamide (ACTZ) were obtained from Sigma (St. Louis, MO). 4,4'-diisothiocyano-2,2'-stilbene disulfonate (DIDS), fluorescein-ovalbumin and Texas Red sulfonamide [1H,5H,11H, 15H-xantheno(2,3,4-ij:5,6,7-i'j')-diquinolizin-18-ium,9-(2(or-4)-((5-aminopentyl)sulfonamido)-4(or-2)-sulfophenyl)-2,3,6,7,12, 13,16,17-octahydro-,hydroxide,inner salt] were supplied by Molecular Probes (Junction City, OR). 4-chlorobenzene sulfonate and 3-nitrobenzene sulfonate were supplied by Aldrich (Milwaukee, WI). All other reagents were from Fisher Scientific (Medford, MA). Outdated blood was kindly supplied by the Children's Hospital (Boston, MA). The concentration of bovine CA solutions was determined by weight, following the manufacturer's specifications that the product was 90% protein and assuming that the only protein was carbonic anhydrase.

Methods

Experiments on BCA II in free solution or in the reconstituted (white) ghost system were performed on a Dionex D-130 stopped-flow photometer (Sunnyvale, CA), which has a dead-time of 2 msec. The analog data were digitized and averaged by a Hewlett-Packard Model 217 computer which was also used for the data analysis. Equal volumes of solutions containing either ghosts (4–8% v/v before mixing), or buffer, and DNSA were mixed and the time course of fluorescence enhancement (excitation 330 nm, emission > 400 nm) was measured. At each DNSA concentration, the contribution of free DNSA fluorescence was subtracted from the enhanced fluorescence. We determined that, at a fixed [DNSA] where [DNSA] ≫ [BCA II], fluorescence amplitude was linearly related to [BCA II]. For each mixing solution, five or more consecutive runs were averaged to improve the signal to noise ratio. All stopped-flow experiments were carried out at room temperature, 23–25°C.

Reconstituted white ghosts were prepared from outdated blood, after aspiration of plasma and buffy coat. The cells were washed three times with PBS (0.15 M NaCl, 5 mM Na_2HPO_4, pH 8.0). Cells were then treated with DIDS, as described below, or were used directly for ghost preparation. Washed red cells were resuspended to 25% hematocrit in PBS, pH 7.4, with (or without) the indicated DIDS concentration and incubated at 37°C for one hour. Cells were then centrifuged, washed with 25 volumes of PBS, pH 8.0, + 0.5% bovine serum albumin (BSA), followed by two more washes with PBS without BSA. Cells were then hemolyzed in 25 volumes of ice-cold 5 mM Na_2HPO_4, pH 8 (lysis buffer), pelleted, and washed an additional three times in this buffer (at 4°C) to yield white ghosts. Ghosts were then resuspended with five volumes of PBS, pH 8, + 100 μM BCA II and incubated for one hour at 37°C to seal them, followed by three washes (25 volumes each) in PBS, pH 8, 4°C, and final resuspension for stopped-flow experiments at room temperature.

One-step (pink) ghosts were prepared by hemolysis in 20 volumes of lysis buffer. Ghosts were pelleted and immediately resuspended in five volumes of PBS, pH 7.4, and incubated for one hour at 37°C. This was followed by two washes in PBS, pH 7.4, and final resuspension in PBS (approx 5% v/v before mixing) for stopped-flow measurements at room temperature.

Treatment with DIDS consisted of a one-hour incubation at 37°C with the indicated [DIDS] of the resealed pink ghost suspension (1 : 20 v/v), which was then used for the stopped-flow measurements, without further washing. The benzene sulfonate experiments were performed by suspending the pink ghosts (1 : 20 v/v) in buffers in which the benzene sulfonates replaced the appropriate concentration of NaCl to maintain osmolality (DNSA solutions were also prepared in these buffers).

All measurements on one-step ghosts were performed with a single beam spectrophotometer (Photon Technology International, South Brunswick, NJ) which uses a reference channel quantum counter for signal normalization. The observation cuvette (vol: 400 μl) is part of a temperature controlled stopped-flow apparatus (model SFA-11, Hi-Tech Scientific, Salisbury, UK). The dead-time, which is governed by the software of the data acquisition system supplied with the Photon Technology instrument, is of the order of 100 msec.

DNSA fluorescence enhancement was determined by excitation at 330 nm (resolution 4 nm) and emission at 460 nm (resolution 4 nm). DNSA was added from a stock 1 mM solution (10 mM HCl, 0.15 M NaCl). Free DNSA fluorescence was monitored by excitation at 330 nm (resolution 4 nm) and emission at 580 nm (resolution 4 nm). Experiments on BCA II in free solution were also performed on the Photon Technology instrument in addition to the Dionex measurements.

Enzymatic activity of BCA II was determined by the method of Thorslund and Lindskog (1967), and is based on the hydrolysis of *p*-nitrophenyl acetate monitored at 348 nm. Enzyme (approx 50 μg/ml) was added to 10 mM TRIS-H_2SO_4 at pH 7.6 (± DIDS). Substrate was added to a final concentration of 0.4 mM, and the reaction was followed for 4 min. A blank without enzyme was determined and the rate of the uncatalyzed reaction was subtracted from the total rate. Activity was calculated from the initial rate of the reaction.

Frozen-thawed ghosts were produced by resuspending

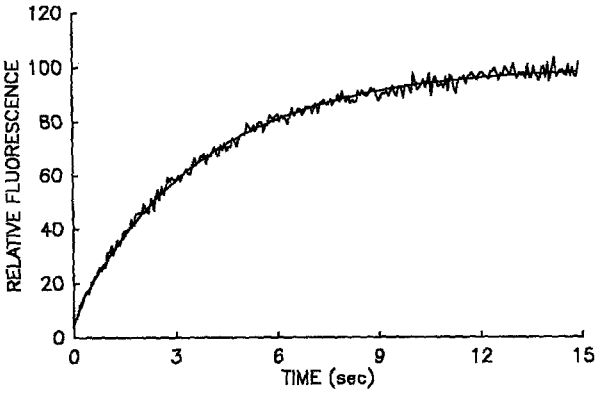

Fig. 1. Time course of 1 μM DNSA binding to one-step (pink) ghosts. Equal volumes of ghosts (1 : 20 v/v) and 2 μM DNSA in PBS, pH 7.4, were mixed and the fluorescence enhancement monitored at 460 nm. The data have been fit to a single exponential with $\tau = 3.77 \pm 0.07$ sec.

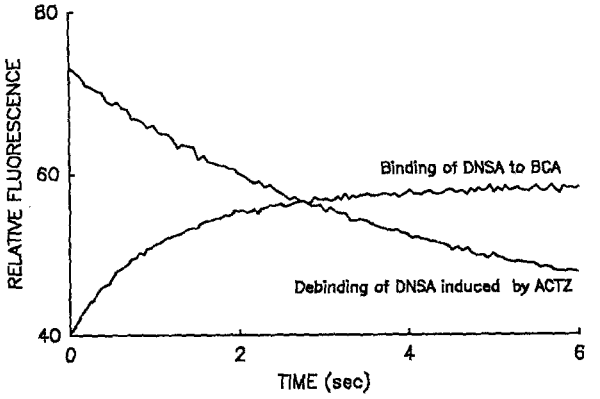

Fig. 2. Bottom curve: binding of 1 μM DNSA to 1 μM BCA II in free solution. Equal volumes of 2 μM DNSA and 2 μM BCA II in PBS, pH 8.0, were mixed in the Dionex apparatus and the time course of fluorescence enhancement was fit to a single exponential with $\tau = 1.1 \pm 0.01$ sec. Upper curve: reversal of DNSA binding by 10 μM ACTZ. Equal volumes of a 2 μM DNSA/2 μM BCA II complex at equilibrium and 20 μM ACTZ, in PBS, pH 8.0, were mixed and the decrease in fluorescence was fit to a single exponential with $\tau = 3.8 \pm 0.03$ sec. Origins of the curves have been shifted to make this display.

ghosts to approximately 80% v/v in PBS and subjecting them to three cycles of freezing at -10°C in an ice water/NaCl bath and thawing at 37°C in a shaking water bath.

Fluorescein conjugated ovalbumin (Fl-OV) fluorescence was excited at 494 nm and measured through a 530 nm bandpass filter (emission = 520 nm) in the Dionex instrument. Our measurements showed that fluorescence amplitude was linear with [Fl-OV] at concentrations less than 0.3 μM. Ghosts were prepared, sealed, and washed after resealing, as in the BCA II reconstitution experiments, except that the [Fl-OV] added at the resealing step was 12 μM, resulting in an average incorporation of 5–6 μM Fl-OV. Ghosts were then appropriately diluted (approx. 1 : 20 v/v) in PBS so that measurements would be in the linear concentration-dependence range.

Kinetics

The fluorescence enhancement is plotted as a function of time, as shown in Fig. 1, and fitted by nonlinear least squares to a single exponential of the form $a(1)e^{-t/\tau} + a(2)$. The pre-exponential, $a(1)$, the fluorescence enhancement of bound DNSA at equilibrium, and the time constant, τ, are the two experimental variables which are obtained directly from the fitted curve and are transformed into k_l and $K_{D,app}$, the parameters which we used to characterize the DNSA/CA association. The forward rate constant, k_l, is computed from τ according to Eq. (2) in the next section. The apparent ligand binding constant, $K_{D,app}$, is obtained by plotting $a(1)$ as a function of ligand concentration as shown in Fig. 7, in which the data are fitted by nonlinear least squares to a single-site binding curve, of the form: $Y = b(2)X/(b(1) + X)$ in which X is the ligand concentration, $b(1) = K_{D,app}$ and $b(2)$ is a fitting parameter. This treatment is applicable when the amount of ligand in the system is great enough, compared to the amount of binding protein, that total ligand concentration essentially equals free ligand concentration. When we are unable to determine the concentration of CA, as in experiments with HCA retained in pink ghosts, we cannot determine whether total ligand equals free ligand. In these cases, $K_{D,app}$ is used as an empirical measure of DNSA/CA binding for comparison with controls obtained under similar conditions. Errors are given as $\pm$SD.

Results and Discussion

Properties of Carbonic Anhydrase in Beef and Human Red Cells

Sulfonamides, which are the classical inhibitors of CA activity, are characterized by a broad range of K_I's, ranging from 2 nM for the important CA inhibitor, ethoxzolamide, to 50 μM for sulfanilamide (inhibition of HCA I, Maren & Sanyal, 1983). The fluorescent sulfonamide, DNSA, was first used by Chen and Kernohan (1967) in experiments on beef CA. They reported that K_D for DNSA/CA binding = 0.24 ± 0.01 μM at pH 7.4 for the purified bovine carbonic anhydrase (BCA II) used in their experiments. DNSA bound with 1 : 1 stoichiometry and inhibited esterase activity with $K_I = 0.4$ μM. Chen and Kernohan showed that DNSA can be completely displaced by ethoxzolamide, whose binding constant, $K_D = 0.25$ nM, is three orders of magnitude tighter, showing that DNSA binds to the inhibitor site. We find that $K_{D,app} = 0.28 \pm 0.10$ μM (6 expts.) for DNSA binding to the commercial BCA II preparation that we have used, in good agreement with Chen and Kernohan (1967). Figure 2 shows the time course of 1 μM DNSA binding to 1 μM BCA II with $\tau = 1.1 \pm 0.01$ sec. Figure 2 also shows that DNSA

is easily displaced by 10 μM ACTZ, for which Lindskog (1963) has determined that $K_D = 0.008$ μM for bovine CA.

The heterogeneity of human CA makes comparisons with the literature difficult. In the human red cell 86.6% of the CA is present in the low activity form, HCA I, and 13.4% is HCA II (Carter et al., 1984); the relative anhydrase activity of HCA II is from 4–15 times that of HCA I (Maren, 1967). The affinity of ligand binding to CA depends upon the specific isozyme/inhibitor couple. For example, Taylor, King and Burgen's (1970) measurements of DNSA binding provide an instance in which HCA II, the high anhydrase activity isozyme, has the lower affinity for DNSA, in contrast to the more usual situation in which the higher inhibitory affinity is associated with the isozyme with the higher anhydrase activity. For HCA II, Taylor et al. (1970) reported that $K_{D,\mathrm{DNSA}} = 1.7$ μM, as compared to $K_{D,\mathrm{DNSA}} = 0.22$ μM for HCA I. In our experiments with hemolyzed human red cells, which contain both HCA I and HCA II, we determined that $K_{D,\mathrm{app}} = 0.10 \pm 0.05$ μM (4 expts.), similar to $K_{D,\mathrm{DNSA}}$ for the high affinity (low activity) HCA I site. This agreement seems reasonable since the HCA I site comprises more than 85% of the total and the DNSA affinities to HCA I and HCA II are relatively close.

Binding Kinetics

As suggested by Taylor et al. (1970) and supported by King (1976), the kinetics of sulfonamide inhibitor binding consist of a bimolecular association, followed by a conformational change, as expressed below for DNSA:

$$\mathrm{DNSA} + \mathrm{CA} \underset{k_{-1}}{\overset{k_1}{\rightleftharpoons}} \mathrm{DNSA\text{-}CA} \underset{k_{-2}}{\overset{k_2}{\rightleftharpoons}} \mathrm{DNSA\text{-}CA^*} \quad (1)$$

in which * denotes the complex after the conformational change. The kinetics of such a sequential reaction scheme can be solved simply in two cases: if the bimolecular association is either very fast or very slow, compared to the conformational change. In the first case, the velocity reaches a maximum at high ligand concentrations, as we observed for DBDS (4,4′-dibenzamido-2,2′-stilbene disulfonate) binding to band 3 (Verkman, Dix & Solomon, 1983). In the second case, the velocity depends linearly upon ligand concentration, and can be described by the following equation, given by Czerlinski (1966):

$$\tau^{-1} = k_1[\mathrm{DNSA}] + k_{-1}/(1 + K_2) \quad (2)$$

which is applicable if the concentration of one of the reactants, in our case DNSA, is large compared to CA, or if the suspension is buffered by a large amount of DNSA, as is also the case in our experiments. $K_2 = k_2/k_{-2}$, the association constant for the conformational change. Figure 3 shows that τ^{-1} depends linearly on DNSA concentrations from 1 to 10 μM for CA concentrations varying between 0.1 and 1.0 μM, consistent with Eq. (2). Since we do not have an independent method for determining K_2, k_1 is the only kinetic constant that can be extracted from Eq. (2). Taylor et al. (1970) analyzed the kinetics of DNSA binding to HCA II, the human enzyme whose properties approximate BCA II, according to the simple bimolecular association model. They reported that $k_1 = 0.24$ $\mu\mathrm{M}^{-1}$ sec^{-1}, not far different from our value of 0.48 ± 0.01 $\mu\mathrm{M}^{-1}$ sec^{-1} for commercial BCA II, derived from Fig. 3, indicating that the resemblance between BCA II and HCA II extends to the kinetics of DNSA binding. We have also determined the kinetics of DNSA binding to pink ghosts in one experiment and have found that $k_1 = 0.31 \pm 0.01$ $\mu\mathrm{M}^{-1}$ sec^{-1} in very good agreement with Taylor et al. (1970). When equilibrium has been reached, the interaction between DNSA and CA can also be characterized by $K_{D,\mathrm{app}}$, the apparent binding constant. $K_{D,\mathrm{app}}$ is obtained by plotting the equilibrium fluorescence enhancement of the bound DNSA, as a function of DNSA concentration, as described in Materials and Methods.

In the early phases of the project we experienced great difficulties in measuring DNSA binding kinetics in human red cells because there is a large and broad hemoglobin (Hb) absorbance peak at about 430 nm, not far from the 460 nm emission peak that

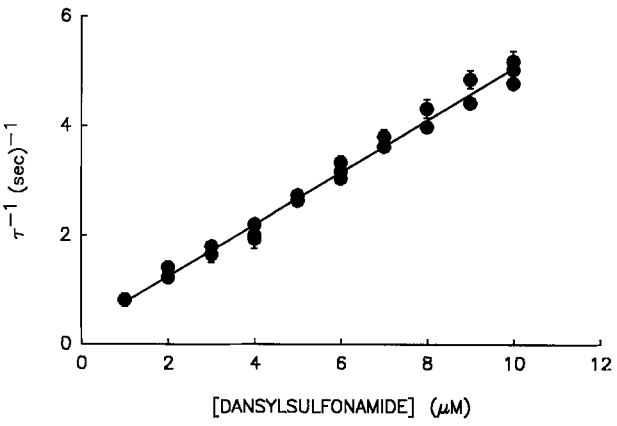

Fig. 3. Dependence of τ^{-1} for DNSA binding to BCA II in free solution, as a function of [DNSA]. Conditions as in Fig. 2 except that [DNSA] $\gg$ [CA] for all measurements. The line has been fit by nonlinear least squares with slope $= 0.48 \pm 0.01$ $\mu\mathrm{M}^{-1}$ sec^{-1} and intercept $= 0.29 \pm 0.08$ sec^{-1}. Data from two experiments (three at some concentrations), varying the BCA II concentration from 0.1 to 1.0 μM. When error bars are not shown, they are within the points.

we use in determining DNSA. In an attempt to find an inhibitor with appropriate spectral qualities, Molecular Probes kindly synthesized Texas Red sulfonamide for us, but this compound does not bind specifically to CA, presumably because the size of the large Texas Red moiety makes the inhibitor too large to permeate the small inhibitor cavity in CA. We then turned to reconstituted white ghosts which are free, not only of Hb, but also of endogenous HCA. It proved impossible to elute Hb without also eluting HCA, which is not surprising in view of the binding that has been observed between Hb and HCA II (Backman, 1981). We would have liked to study a reconstituted system in which HCA II was incorporated into resealed white ghosts, but the cost of HCA made this impossible. The next best alternative was to reconstitute BCA II, which was affordable, into resealed white ghosts.

Permeability of Ghosts to Sulfonamides

Since extracellular DNSA has to traverse the cell membrane to bind to cell CA, it is necessary to determine whether cell membrane permeability affects DNSA/CA binding kinetics. The importance of lipid solubility as a determinant of sulfonamide permeation of red cells was clearly shown by Holder and Hayes (1965). They compared the permeation of red cells by ethoxzolamide and ACTZ, molecules of roughly equivalent size but vastly different lipid solubility. In their units, the permeability coefficient, P_{ub}, is 4,500 hr^{-1} for ethoxzolamide as compared to 27 hr^{-1} for ACTZ; the $CHCl_3/H_2O$ partition coefficient is 25.0 for ethoxzolamide as compared to 0.001 for ACTZ. The lipid solubility of DNSA makes its permeation very much faster than ACTZ, as shown by an experiment in which we measured the debinding of DNSA from DNSA/CA in pink ghosts suspended in a DNSA-free buffer and found $\tau = 6.6 \pm 0.7$ sec, not significantly different from the debinding time constant in hemolyzed ghosts, 8.1 ± 0.7 sec. This shows that DNSA permeation of the ghost membrane has no detectable effect on DNSA binding kinetics.

Resealed white ghosts, prepared by the method of Steck and Kant (1974), upon which our method of preparation is based, are characterized by a single membrane hole with a diameter of 30–40 Å, and resealed pink ghosts have a smaller membrane hole with a diameter of about 18 Å (Lieber & Steck, 1982). Since the planar dimensions of DNSA, measured on CPK models, are approximately 8.8×12.4 Å and the molecule is about 6 Å thick, DNSA should be able to permeate white ghosts through the hole, and ACTZ, which is smaller, should be able to permeate pink ghosts. Nonetheless, pink ghosts offer considerable impedance to ACTZ permeation. We used a method based on the time course of DNSA debinding to measure the time course of ACTZ permeation in two experiments and found that τ is 112 sec in pink ghosts as compared to 25 sec in hemolyzed red cells.

Does Cell CA Interact with Membrane Constituents?

CA can interact with the cell membrane either mechanically, by entrapment in the membrane cytoskeleton, or chemically, by binding to a protein or other component of the membrane. Parkes and Coleman (1989) have shown that BCA II can react with human red cell membrane fragments to form a complex which exhibits enhanced catalytic activity, as shown by increases in both K_m and V_{max}, not only for BCA II, but also for HCA II. The membrane proteins in the Parkes and Coleman preparation may not have remained in their native state since the membranes had been prepared by five sonications following eight washes in 10 mM HEPES buffer. Nonetheless, the CA remained bound to the membrane after centrifugation through a sucrose density gradient and Parkes and Coleman showed that CA could be cross-linked to the red cell membrane, though there was no evidence of specific association with any red cell protein.

In the course of our studies with BCA II, which is the predominant and probably the only CA in bovine red cells, we learned that the only way to incorporate BCA II in ghosts was to incorporate it at the time of resealing. BCA II would not diffuse into unsealed ghosts and remain in place after washing. However, when BCA II was placed in the resealing solution, incorporation of BCA II depended smoothly on the BCA II concentration. There was no binding of BCA II to the outside face of resealed ghosts.

We next carried out a series of experiments to see how tightly the reconstituted BCA II was held by the ghost. For this purpose, we created large holes in the membrane by subjecting the reconstituted sealed ghosts to three freeze-thaw cycles. We established that the apertures caused by the freeze-thaw procedure were large enough to permit passage of BCA II by washing the resealed ghosts with water to remove both the cytoskeleton and the remaining cell contents. After this treatment no incorporated BCA II remained. On the other hand, washing at high ionic strength with PBS removes a variable amount, from 10–35%, of the BCA II, leaving the rest firmly bound, impervious to further PBS washes

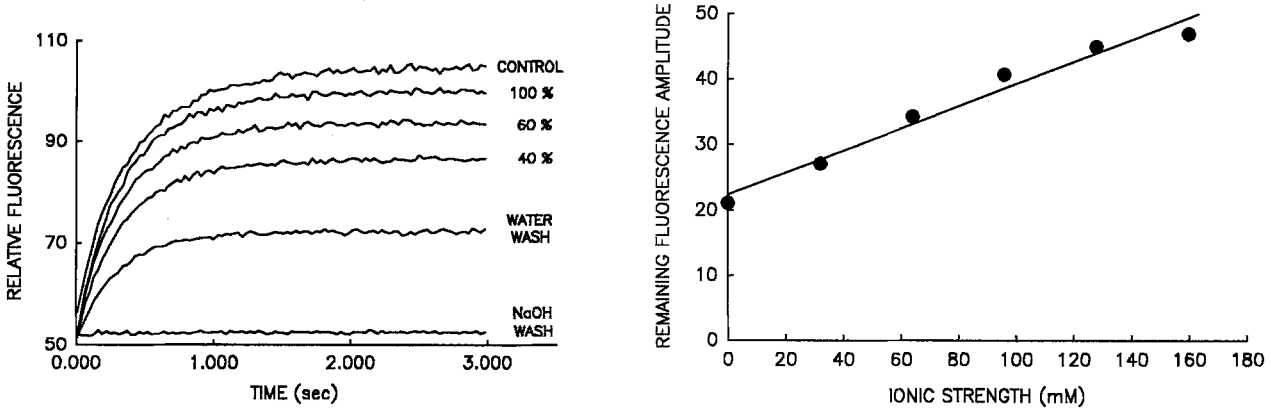

Fig. 4. (Left) Ionic strength dependence of the elution of reconstituted BCA II from frozen/thawed resealed ghosts. Ghosts were washed with 5 volumes of the ionic strength shown next to the curves (100% = 0.16 M, control = unwashed ghosts) and resuspended with 5 volumes of PBS, pH 8, for mixing. DNSA = 5 μM, final concentration. NaOH wash was with 0.1 N NaOH. (Right) Fluorescence amplitudes (proportional to [BCA II] at a fixed [DNSA] $\gg$ [BCA II]) plotted as a function of ionic strength wash. The line has been fit by nonlinear least squares with intercept = 22.3 $\pm$ 1.4 fluorescence units and slope = 0.272 $\pm$ 0.02 fluorescence units/mM ionic strength.

(up to four additional washes). In order to remove the remaining bound 65–90% of the BCA II, it was necessary to wash with lower ionic strength. Figure 4 (left) shows how the retained CA is released as the reconstituted ghosts are washed with buffers of decreasing ionic strength (volume ratios of 5 : 1). After the water wash, 45% of the BCA II remained (relative to the curve marked 100% in Fig. 4, left) which can be reduced to zero by a subsequent water wash with a volume ratio of 50 : 1.

The concentration of BCA II retained following the first PBS wash is smoothly dependent upon the ionic strength of the wash solution as shown in Fig. 4 (right). The ability of 0.1 N NaOH to remove the cytoskeleton is illustrated by the fact that a single wash with 0.1 N NaOH removes the remaining 45% of the bound BCA II. These observations suggest that the BCA II is caught up in the cytoskeleton, since the low ionic strength and NaOH washes which remove the cytoskeleton (Steck & Yu, 1973) remove the BCA II, and those that leave the cytoskeleton intact, such as further washes with the high ionic strength buffer, have no further effect on BCA II elution.

In order to see whether the retention of BCA II depended upon specific characteristics of the enzyme or was a generalized phenomenon that would apply to other proteins, we carried out a control experiment using fluorescein-labeled ovalbumin. We chose ovalbumin because its size was comparable to CA [CA: 30,000 D, $\bar{V}$ = 0.742 ml gm^{-1}; ovalbumin; 45,000 D, $\bar{V}$ = 0.748 ml gm^{-1}] (Maren, 1967; Tanford, 1967). We found no striking difference between ovalbumin and BCA II. Ninety percent of the fluorescein-ovalbumin was retained after the first two PBS washes. After an additional water wash 50% remained, which was reduced to 10% after a second water wash. These experiments indicate that, as far as dependence on ionic strength is concerned, a very large fraction of BCA II retention is similar to that of ovalbumin and is consistent with some generalized protein interaction with the cytoskeleton.

Effect of DIDS on DNSA/CA Binding

The observation that BCA II can be removed from white ghosts at low ionic strength does not mean that there is no association at physiological ionic strength. The probe that we used to look for such an association was the conformation changes in band 3 that are induced by covalent reaction with DIDS. Observation of an allosteric change in DNSA/CA binding kinetics subsequent to DIDS/band 3 reaction would serve as evidence of an interaction between band 3 and CA. The specificity of DIDS binding to band 3 was established by Ship et al. (1977), who showed that 90% of covalently bound DIDS (10 μM) was bound to band 3 and that anion efflux declined linearly with DIDS concentration over the range of 0–9 μM DIDS. We had previously shown (Fossel & Solomon, 1981) that extracellular DIDS induces a change in the conformation of the glycolytic enzyme, glyceraldehyde-3-phosphate dehydrogenase, which has a well-defined binding site on the cytosolic pole of band 3 (Low, 1986). DIDS also alters the conformation of the membrane-bound red

Table 1. Effect of 1.2 μM DIDS on DNSA/HCA binding kinetics[a]

Experimental condition	Expt.	$k_{1,DIDS}/k_{1,control}$	$K_{D,app,control}$	$K_{D,app,+DIDS}$
			μM DNSA	μM DNSA
Covalent DIDS	1	1.32 ± 0.09		
	2	1.04 ± 0.05		
	3	1.35 ± 0.06	0.15 ± 0.03	0.26 ± 0.04
	4	1.05 ± 0.05	0.19 ± 0.02	0.27 ± 0.05
	5	1.15 ± 0.04	0.16 ± 0.01	0.22 ± 0.01
Ave ± SD		1.18 ± 0.15	0.17 ± 0.02	0.25 ± 0.03
Noncovalent DIDS		1.02 ± 0.01		
Free solution[b]		1.02 ± 0.05		

[a] The data for expt. 3 are shown in Fig. 6, in which the 100% line is that for 1.2 μM DIDS. The data for expt. 5 are those in Fig. 7 in which the pooled values were used for the 1.2 μM DIDS figure. The data for columns 3 and 4 were obtained in the same experiments used for column 2.
[b] DIDS 10 μM; there was also no effect on enzyme activity which was 0.046 ± 0.001 min^{-1} in the control as compared to 0.047 ± 0.002 min^{-1} in the presence of DIDS (3 expts.).

cell glucose transport protein (Janoshazi et al., 1991). Hb also binds to the cytosolic domain of band 3 and Salhany, Cordes and Gaines (1980) have shown that DIDS alters Hb affinity.

Our initial DIDS studies were carried out to determine whether reaction of DIDS with band 3 would alter the kinetics of DNSA binding to BCA II incorporated into white ghosts. Cells were reacted covalently with DIDS before reconstitution, and k_1 for DNSA/BCA II binding was measured as a function of DIDS concentration (expressed as mol DIDS bound/mol band 3). We first determined that 10 μM DIDS had no effect either on the time course of DNSA/BCA II binding in free solution or on BCA II enzymatic activity, as shown in the bottom line of Table 1. In resealed white ghosts, however, k_1 increases regularly with the fraction of band 3 that has reacted with DIDS, as shown by the results of the two pooled studies in Fig. 5. The dependence can be described empirically by a binding curve which saturates when all of the band 3 has reacted with DIDS (DIDS/band 3 = 1.0) at $k_1 = 0.6\ \mu M^{-1}\ sec^{-1}$. These results show that the conformational change in band 3 subsequent to binding of DIDS on the extracellular face of the reconstituted ghost leads to a change in the conformation of BCA II as evidenced by the altered kinetics of DNSA binding.

The next set of experiments were designed to determine whether a similar effect can be observed in pink ghosts, in which some native HCA is also retained, along with the Hb. The experiments in Fig. 6 show a covalent-DIDS-induced stimulation of the rate of rise of τ^{-1}, whose dependence on [DNSA] increases with the fraction of band 3 reacted with DIDS. There was no effect with noncovalent DIDS,

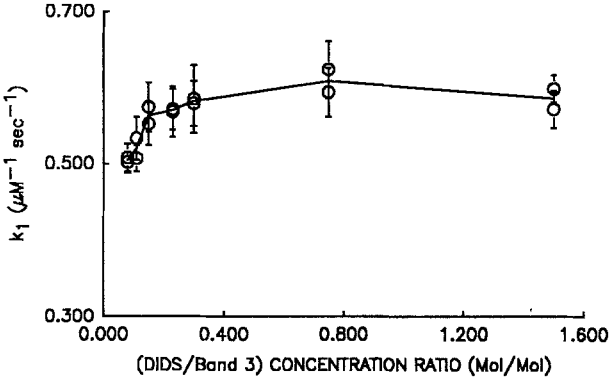

Fig. 5. Effect of DIDS on DNSA binding kinetics in ghosts reconstituted with BCA II. The forward rate constant, k_1, is plotted as a function of the ratio (mol DIDS added/mol band 3). The midpoints of the data pairs have been joined by straight lines. The data may also be fit empirically by nonlinear least squares to a single-site binding curve with maximum $k_1 = 0.61 \pm 0.008\ \mu M^{-1}\ sec^{-1}$.

as shown in Table 1. The value for k_1, determined from the slopes of the lines relating τ^{-1} to DNSA concentration in Fig. 6, increases with the fractional amount of band 3 reacted covalently. The control k_1 ($0.31 \pm 0.02\ \mu M^{-1}\ sec^{-1}$) rises to $0.38 \pm 0.01\ \mu M^{-1}\ sec^{-1}$ at 50% reaction (difference from control, $P < 0.01$, t-test) and to $0.43 \pm 0.02\ \mu M^{-1}\ sec^{-1}$ for 100% reaction (difference from 50%, $P < 0.02$, t-test). We also studied intermediate concentrations ranging from 10 to 75% and found an orderly increase in k_1 with increases in the fraction of band 3 reacted.

The DIDS-induced conformation change in HCA is also evidenced in a decreased binding affinity, as shown in Fig. 7 by the rise in $K_{D,app}$ from a

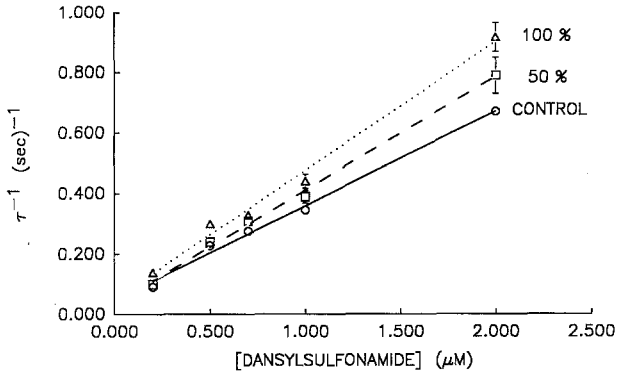

Fig. 6. Effect of covalent DIDS on DNSA binding kinetics in pink ghosts. Ghosts (1 : 20 v/v, [band 3] = 1.2 μM at this dilution) were incubated at 37°C for 1 hr with either 1.2 μM DIDS (100% mol DIDS/mol band 3) or 0.6 μM DIDS (50%), and the binding kinetics for the indicated DNSA concentrations was measured as in Fig. 1. For the control (○), slope = 0.31 ± 0.02 μM^{-1} sec^{-1}; for 50% DIDS/band 3 (□), slope = 0.38 ± 0.01 μM^{-1} sec^{-1}; for 100% DIDS/band 3 (△), slope = 0.43 ± 0.02 μM^{-1} sec^{-1}. When the error bars are not shown, they are within the points.

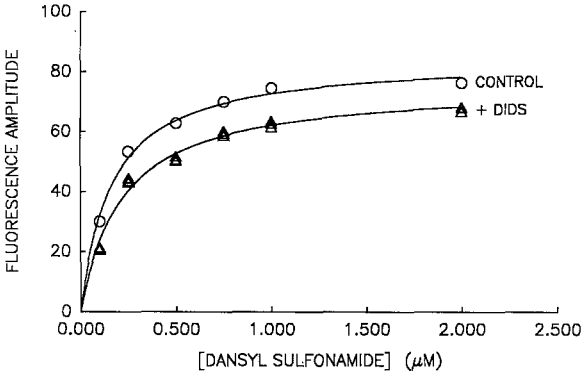

Fig. 7. Saturation of the DIDS effect on DNSA binding to pink ghosts, as measured by signal amplitude. Fluorescence amplitudes fit to single-site binding curves. Data for DIDS experiments (100, 150 and 200% mol/mol [DIDS]/[band 3]) were pooled and fit to a single curve. For the control, $K_{D,app}$ = 0.16 ± 0.01 μM and for the pooled DIDS curves, $K_{D,app}$ = 0.22 ± 0.01 μM. Error bars are within the points.

control value of 0.16 ± 0.01 μM to 0.22 ± 0.01 μM, after covalent reaction with DIDS. The difference between these two values of $K_{D,app}$ is significant at $P < 0.01$ (t-test). Since the DIDS figure is a pooled value for all the DIDS concentrations sufficient to react with 100, 150 and 200% of the band 3, this experiment shows that the effect saturates when all the band 3 has reacted with DIDS. A similar saturation effect was observed using k_1 as an index. Since nonspecific adsorption would not saturate, these experiments confirm our attribution of the DIDS effect to a specific reaction with band 3.

Table 1 gives the results of five experiments (including the two above) with 1.2 μM DIDS, which is the DIDS concentration required for mol/mol reaction with the band 3 in our pink ghosts. The average k_1 ratio of 1.18 ± 0.15 is different from 1.0 at $P \approx 0.05$, t-test [the t value for $P = 0.05$ is 2.776; our t is 2.773]. As Table 1 shows, there is a great deal of variability between experiments and for experiments 2 and 4 there is no effect of covalent DIDS on the $k_{1,DIDS}/k_{1,control}$ ratio. In the last three of the experiments in the Table, we extended the DNSA concentration range to include points at low [DNSA], so that we could also determine $K_{D,app}$, as was done for expt. 5, which is the control curve in Fig. 7. Table 1 shows that there is a comparable increase in experiments 3 and 4. The error-weighted average of the ratio, $K_{D,app,DIDS}/K_{D,app,control}$, is 1.41 ± 0.06 for experiments 3, 4 and 5, which differs significantly from 1.0 ($P < 0.01$, t-test), confirming the effect of DIDS on the DNSA/HCA binding constant. Taken together with the effects in Figs. 6 and 7, these experimental results show that DIDS interaction with band 3 modulates the kinetics of DNSA binding to HCA in pink ghosts.

Effect of Benzene Sulfonate Inhibitors on DNSA/HCA Binding

In the course of their extensive study of the chemical properties of red cell anion recognition sites, Barzilay et al. (1979) characterized congeners of both benzene sulfonic acids (BS) and stilbene sulfonic acids (DS). Although the ID_{50}'s for anion exchange inhibition were in the μM range for DS and in the mM range for BS, Barzilay et al. (1979) found that both BS and DS had a common site of action on the anion channel. Barzilay and Cabantchik (1979) chose to characterize the nitroaromatic sulfonic acids (3-nitrobenzene sulfonate, 3NBS, and 4,4′-dinitro-2,2′-stilbene disulfonate, DNDS) to make their detailed and comprehensive comparison of the properties of the BS and DS inhibitors. They found that both 3NBS and DNDS act on the transport site of anion exchange and that the inhibition of each congener is competitive.

In our study of BS effects on red cell water and urea permeability, we found (Solomon & Toon, 1992) that one of the organic sulfonates, 4-chlorobenzene sulfonate (4CBS), inhibits red cell urea permeability by up to 94%, while stimulating water permeability by up to 46%. Benzene sulfonate (BSate) has similar, but smaller effects. These organic sulfonate effects on red cell urea and water permeability are much larger than those exercised by DIDS, which has been shown to have no effect on red cell

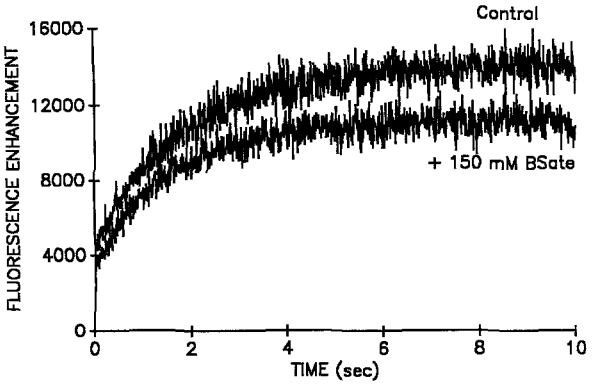

Fig. 8. Effect of benzene sulfonate on DNSA binding to bovine carbonic anhydrase in free solution. DNSA and CA solutions were prepared in either PBS, pH 7.4, (top curve) or 150 mM BSate (sodium salt), 5 mM Na_2HPO_4, pH 7.4, (bottom curve). [DNSA] = 2 μM and [CA] = 0.5 μM after mixing. $\tau_{control}$ = 1.6 ± 0.1 sec; τ_{BS} = 1.8 ± 0.1 sec.

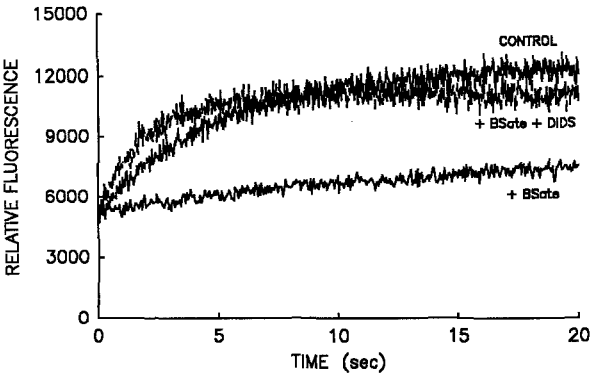

Fig. 9. Effect of 75 mM benzene sulfonate on DNSA binding to pink ghosts. Pink ghosts were treated with 1.5 μM DIDS in PBS for one hour at 37°C before resuspension in benzene sulfonate buffer for stopped-flow measurements. [DNSA] = 1 μM. τ_{cont} = 4.9 ± 0.4 sec; τ_{BSate} = 21.4 ± 1.1 sec; $\tau_{BSate+DIDS}$ = 5.0 ± 0.2 sec.

urea permeability while stimulating water permeability by up to ≈ 20% (M.R. Toon and A.K. Solomon, *unpublished*). Somewhat to our surprise, the BS inhibitors exercise much more profound effects on DNSA/HCA binding kinetics than do the DS. Despite the lack of a sulfonamide group in BSate, there is a superficial resemblance between BSate and the sulfonamides, so it was necessary to determine whether there was any direct effect of BSate on DNSA binding to BCA II in free solution, before embarking on DNSA/HCA binding studies. The control experiment in Fig. 8 shows that 150 mM BSate has a relatively small effect (12.5%) on the time course of 2 μM DNSA binding to 0.5 μM BCA II in free solution; a similar result[1] was found with 25 mM 4CBS. In pink ghosts, however, 75 mM BSate caused a very large increase in the time constant, τ, for DNSA/HCA binding, which went up by a factor of four, from 4.9 ± 0.4 to 21.4 ± 1.1 sec, as shown in Fig. 9. In view of the competitive inhibition of DS and BS congeners for the anion exchange inhibition site that Barzilay and Cabantchik (1979) had reported, we expected that covalent reaction of DIDS to band 3 would block the anion exchange site. Thus, BSate would no longer be able to bind to its site on band 3 so that it could no longer modify the τ for DNSA/CA binding. The data in Fig. 9 show this to be the case, since covalent DIDS decreases τ from 21.4 ± 1.1 sec, as given above, back down to 5.0 ± 0.2 sec, for the curve marked *+BSate + DIDS*. This finding shows that BSate binding to the DIDS site is responsible for the observed increase in τ. The small remaining inhibition of the fluorescence enhancement in the presence of DIDS is attributed to the direct DIDS effect on the binding kinetics as was shown in Fig. 7.

Barzilay et al. (1979) measured the inhibitory potency (ID_{50}) of ten BS congeners which varied over two orders of magnitude (0.6 to 61 mM) and found that they were linearly related to the Hammett coefficient, σ, a measure of the negatively charged groups in the molecule. In order to see whether the same factor was involved in the effect on DNSA/CA binding kinetics, we measured the apparent K_I in three experiments with BSate and two experiments with 4CBS. The maximum increase in τ was determined for both BSate and 4CBS, and K_I was then determined by fitting a single-site binding curve (by nonlinear least squares) to the fractional inhibition as a function of BSate and 4CBS concentration, as illustrated for a single experiment in Fig. 10. The average $K_{I,app}$ for BSate is 50 ± 31 mM, and that for 4CBS is 6.0 ± 0.6 mM. These $K_{I,app}$'s differ by an order of magnitude. They are virtually the same as the ID_{50}'s Barzilay et al. (1979) found for anion exchange, both in magnitude and difference, as shown in Table 2. The agreement between these two measures of BS action shows that the same factors that determine the inhibitory potency of anion flux inhibition also govern the BS effect on DNSA/CA binding kinetics.

Our experiments have shown that, far from being an enzyme which diffuses freely in a cytosolic solution, CA is bound in the mesh of structural pro-

[1] We attempted to carry out additional experiments with 3-nitrobenzene sulfonate (3NBS) but were unable to do so because 3NBS interacts with BCA II in free solution. The wide spectrum of compounds that Taylor et al. (1970) and others found to react with CA all contain a sulfonamide group which is lacking in 3NBS, but it is still possible that 3NBS may bind to the same site.

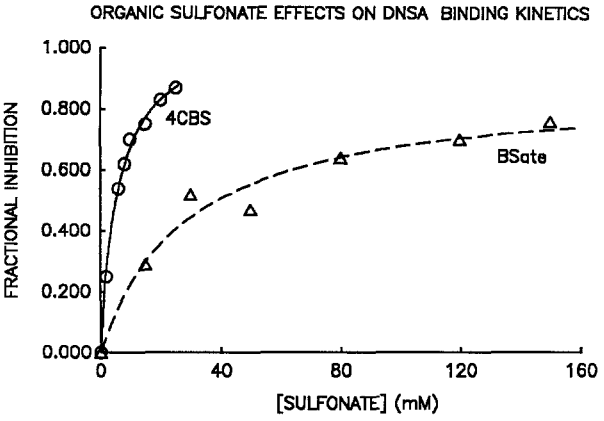

Fig. 10. Dependence of benzene sulfonate effect on DNSA binding kinetics in pink ghosts on [BSate] and [4CBS]. Fractional inhibition is that of τ^{-1}, where the control τ^{-1} is set at zero inhibition. For BSate, $K_{I,app}$ = 34.5 ± 5.1 mM; maximal inhibition = 0.95 ± 0.05. For 4CBS, $K_{I,app}$ = 6.1 ± 0.4 mM; maximal inhibition = 1 ± 0.03.

Table 2. Comparison of organic sulfonate effects on DNSA/CA binding kinetics and anion exchange

Organic sulfonate	DNSA/CA binding kinetics	Anion exchange*
	$K_{I,app}$ mM	ID_{50} mM
Benzene sulfonate (BSate)	50 ± 31	47 ± 15
4-chlorobenzene sulfonate (4CBS)	6.0 ± 0.6	5.5 ± 2.2

* Barzilay et al. (1979).

teins which underlie the membrane. It can only be removed by drastic treatments which disrupt this ordered network. Furthermore, the results of the DIDS and the organic sulfonate experiments, taken together, lead us to conclude that there is a linkage between band 3, presumably via its cytoplasmic pole, and cytosolic HCA, which leads to an allosteric interaction affecting the conformation of the sulfonamide binding site of HCA.

Thus, in this cytosolic array of proteins, CA is constrained to a position in which it can interact with band 3 to carry out CO_2/HCO_3^- hydration most effectively to satisfy the body's needs. We have previously suggested (Solomon, 1992) that band 3, the most abundant integral membrane protein, is the centerpiece of a transport protein assembly which contains the integral membrane proteins, the Na^+,K^+-ATPase and GLUT1, as well as the glycolytic enzyme complex in the cytosol. Low (1986) presents evidence that the cytosolic pole of band 3 is a 250 Å long cylindrical dimer which intersects at its midpoint with the spectrin-actin-ankyrin mesh and extends through the mesh to binding sites for the glycolytic enzymes and Hb at the N-terminus of band 3 deep within the cytosol. Our findings now show that CA is another member of the cytosolic entourage and lead to the suggestion that the cytosol is a strictly ordered assembly that bears much more relation to the spatial organization typical of a biological membrane, albeit a three dimensional one, than to the freedom of motion characteristic of free solution.

Low et al. (1987) showed that binding of the glycolytic proteins, including aldolase and glyceraldehyde-3-phosphate dehydrogenase was controlled by tyrosine phosphorylation of band 3. Subsequently Harrison et al. (1991) showed that this phosphorylation process regulated erythrocyte glycolysis. Our studies (Fossel & Solomon, 1978) showed that the action of the cation transport inhibitor, ouabain, on the extracellular face of red cell Na^+,K^+-ATPase could effect a change in the conformation of glyceraldehyde 3-phosphate dehydrogenase in the cytosol. Clearly, band 3 and its cytosolic pole play, not only a structural, but also a functional role in the supply of metabolic energy and the transport of ions across the red cell membrane. The addition of CA to the roster of transport related proteins with which band 3 interacts is entirely consistent with both of their roles in the transport and metabolism of HCO_3^-.

We should like to express our thanks to Dr. I.M. Wiener for kindly supplying us with the impermeable sulfonamide, ZBI, which we used in preliminary experiments and to Dr. T.H. Maren for analysis of a sample of BCA II.

This work was supported in part by a grant-in-aid from the American Heart Association, by the Squibb Institute for Medical Research and by The Council for Tobacco Research.

References

Backman, L. 1981. Binding of human carbonic anhydrase to human hemoglobin. *Eur. J. Biochem.* **120**:257–261

Barzilay, M., Cabantchik, Z.I. 1979. Anion transport in red blood cells. II. Kinetics of reversible inhibition by nitroaromatic sulfonic acids. *Membr. Biochem.* **2**: 255–281

Barzilay, M., Ship, S., Cabantchik, Z.I. 1979. Anion transport in red blood cells I. Chemical properties of anion recognition sites as revealed by structure-activity relationships of aromatic sulfonic acids. *Membr. Biochem.* **2**:227–254

Carter, N.D., Heath, R., Welty, R.J., Hewett-Emmett, D., Jeffery, S., Shiels, A., Tashian, R.E. 1984. Red cells genetically deficient in carbonic anhydrase II have elevated levels of a carbonic anhydrase indistinguishable from muscle CA III. *Ann. N.Y. Acad. Sci.* **429**:284–286

Chen, R.F., Kernohan, J.C. 1967. Combination of bovine carbonic anhydrase with a fluorescent sulfonamide. *J. Biol. Chem.* **242**:5813–5823

Czerlinski, G.H. 1966. Chemical Relaxation. Marcel Dekker, New York

Fossel, E.T., Solomon, A.K. 1978. Ouabain-sensitive interaction between human red cell membrane and glycolytic enzyme complex in cytosol. *Biochim. Biophys. Acta* **510**:99–111

Fossel, E.T., Solomon, A.K. 1981. Relation between red cell membrane (Na^+,K^+)-ATPase and band 3 protein. *Biochim. Biophys. Acta* **649**:557–571

Harrison, M.L., Rathinavelu, P., Arese, P., Geahlen, R.L., Low, P.S. 1991. Role of band 3 tyrosine phosphorylation in the regulation of erythrocyte glycolysis. *J. Biol. Chem.* **266**:4106–4111

Holder, L.B., Hayes, S.L. 1965. Diffusion of sulfonamides in aqueous buffers and into red cells. *Mol. Pharmacol.* **1**:266–279

Janoshazi, A., Kifor, G., Solomon, A.K. 1991. Conformational changes in human red cell membrane proteins induced by sugar binding. *J. Membrane Biol.* **123**:191–207

Janoshazi, A., Solomon, A.K. 1989. Interaction among anion, cation and glucose transport proteins in the human red cell. *J. Membrane Biol.* **112**:25–37

Jennings, M.L. 1989. Structure and function of the red blood cell anion transport protein. *Annu. Rev. Biophys. Biophys. Chem.* **18**:397–430

King, R.W. 1976. Kinetic aspects of structure-activity relationships in the carbonic anhydrase-sulfonamide system. *In*: Drug Action at the Molecular Level. G.C.K. Roberts, editor. pp. 93–107. University Park Press, Baltimore

Lieber, M.R., Steck, T.L. 1982. Dynamics of the holes in human erythrocyte membrane ghosts. *J. Biol. Chem.* **257**:11660–11666

Lindskog, S. 1963. Effects of pH and inhibitors on some properties related to metal binding in bovine carbonic anhydrase. *J. Biol. Chem.* **238**:945–951

Low, P.S. 1986. Structure and function of the cytoplasmic domain of band 3: center of erythrocyte membrane-peripheral protein interactions. *Biochim. Biophys. Acta* **864**:145–167

Low, P.S., Allen, D.P., Zioncheck, T.F., Chari, P., Willardson, B.M., Geahlen, R.L., Harrison, M.L. 1987. Tyrosine phosphorylation of band 3 inhibits peripheral protein binding. *J. Biol. Chem.* **262**:4592–4596

Maren, T.H. 1967. Carbonic anhydrase: chemistry, physiology, and inhibition. *Physiol. Rev.* **47**:595–781

Maren, T.H., Sanyal, G. 1983. The activity of sulfonamides and anions against the carbonic anhydrases of animals, plants, and bacteria. *Annu. Rev. Pharmacol. Toxicol.* **23**:439–459

Parkes, J.L., Coleman, P.S. 1989. Enhancement of carbonic anhydrase activity by erythrocyte membranes. *Arch. Biochem. Biophys.* **275**:459–468

Randall, R.F., Maren, T.H. 1972. Absence of carbonic anhydrase in red cell membranes. *Biochim. Biophys. Acta* **268**:730–732

Salhany, J.M., Cordes, K.A., Gaines, E.D. 1980. Light-scattering measurements of hemoglobin binding to the erythrocyte membrane. Evidence for transmembrane effects related to a disulfonic stilbene binding to band 3. *Biochemistry* **19**:1447–1454

Schuster, V.L., Bonsib, S.M., Jennings, M.L. 1986. Two types of collecting duct mitochondria-rich (intercalated) cells: lectin and band 3 cytochemistry. *Am. J. Physiol.* **251**:C347–C355

Ship, S., Shami, Y., Breuer, W., Rothstein, A. 1977. Synthesis of tritiated 4,4′-diisothiocyano-2,2′-stilbene disulfonic acid and its covalent reaction with sites related to anion transport in human red blood cells. *J. Membrane Biol.* **33**:311–323

Solomon, A.K. 1992. Interactions between band 3 and other transport-related proteins. *In*: The band 3 proteins: anion transporters, binding proteins and senescent antigens E. Bamberg and H. Passow, editors. Progress in Cell Research, Vol. 2, pp. 269–283, Elsevier, Amsterdam

Solomon, A.K., Toon, M.R. 1992. Organic sulfonates inhibit red cell urea flux and stimulate water flux. *Biophys. J.* **61**:A521

Steck, T.L., Kant, J.A. 1974. Preparation of impermeable ghosts and inside-out vesicles from human erythrocyte membranes. *Methods Enzymol.* **31**:172–180

Steck, T.L., Yu, J. 1973. Selective solubilization of proteins from red blood cell membranes by protein perturbants. *J. Supramol. Struct.* **1**:220–232

Tanford, C. 1967. Physical Chemistry of Macromolecules, Wiley, New York

Taylor, P.W., King, R.W., Burgen, A.S.V. 1970. Kinetics of complex formation between human carbonic anhydrases and aromatic sulfonamides. *Biochemistry* **9**:2638–2645

Thorslund, A., Lindskog, S. 1967. Studies of the esterase activity and the anion inhibition of bovine zinc and cobalt carbonic anhydrases. *Eur. J. Biochem.* **3**:117–123

Verkman, A.S., Dix, J.A., Solomon, A.K. 1983. Anion transport inhibitor binding to band 3 in red blood cell membranes. *J. Gen. Physiol.* **81**:421–449

Zeidel, M.L., Silva, P., Seifter, J.L. 1986. Intracellular pH regulation in rabbit renal medullary collecting duct cells. *J. Clin. Invest.* **77**:1682–1688